3.3 Beam Dynamics

3.3.1 Introduction

To achieve the desired high luminosities, long trains of bunches with very small transverse sizes are required at the interaction point. In this chapter, the issues, pertinent to emittance preservation during the acceleration in the main linac, are discussed. The primary sources of transverse emittance dilution in a high energy linear accelerator are the transverse wakefields excited in the accelerating sections and the dispersive errors caused by the focusing magnets. However, thanks to the low RF frequency and the large iris holes of the TESLA accelerating structure, wakefield effects are much smaller than in higher frequency designs working at room-temperature. Furthermore, the dispersive effects can be easily controlled because the beam energy spread is kept at a small value along most of the accelerator. In turn, that means that the alignment tolerances on the different elements - focusing magnets, beam position monitors, accelerating structures - which are achievable by nowadays survey techniques, are sufficient to ensure beam quality preservation without recourse to other very elaborated and complex correction techniques.

3.3.2 Beam Optics

The focusing of the beam is ensured by means of FODO lattices, which are characterized by the phase advance and the beta function. A constant phase advance of $\mu = 90°$ and an energy scaling of the beta function, $\beta \propto E^{\alpha}$ with $\alpha = 1/2$, are usually chosen. This beta scaling is optimal in the sense that the BNS damping technique, used to suppress the wakefield effect induced by a coherent betatron oscillation, is efficient all along the linac for a bunch of constant correlated energy spread. We will see thereafter that for the TESLA linac, BNS damping is not required because of low wakefields. A larger beta function and a weaker beta scaling with energy, $\alpha = 0$ to 0.2, is more appropriate. The wakefields effects are dominant for large α values (less quadrupoles) whereas the chromatic effects are dominant for small α values (more quadrupoles). The TESLA lattice was then optimized in such a way that a balance of both effects is achieved, leading to the smallest transverse emittance growth. Two beta steps in total, at 50 and 150 GeV, giving minimal emittance growth, are enough. Consequently, the number of matching sections, needed at each beta step, is reduced. On the other hand, at the low energy part of the linac, the focusing lattice must make the best of both TESLA and FEL beams, which have different energies. The difference in energy between the two beams is accomplished by decreasing the accelerating gradient from 25 MV/m to 15 MV/m. A lower phase advance of $\mu = 60°$ for the high energy beam is chosen in order to make the low energy beam stable. The same phase advance is kept all along the linac, because a higher phase advance after the extraction point of the FEL beam does not improve the results. The adopted beta function along the linac of TESLA 500 is shown on Fig. 3.3.1. The linac is divided into 3 sections, with quadrupole spacings of 2, 3 and 4 cryo-modules, respectively. The last quadrupoles

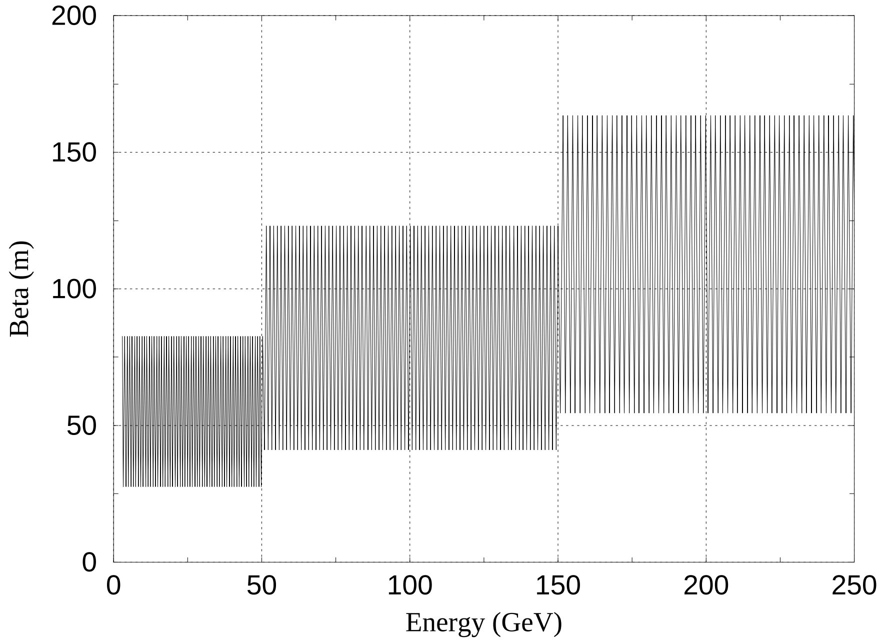

Figure 3.3.1: *Beta function along the TESLA 500 linac.*

located at the high energy part have to provide an integrated field gradient of about 17 T. For superconducting quadrupoles, allowing 1 T fields at the pole, the length of the magnet is still modest. With regard to the beam optics, being faced with the energy upgrade of the linac, the strategy is the following : the beta steps are kept to the same location and the same quadrupole arrangement is used. For TESLA 800, the linac is unchanged till the first beta step, coinciding with the extraction point of the FEL beam. From this 50 GeV point, the accelerating field rises to 40 MV/m and the second beta step occurs now at 210 GeV. For TESLA 1600, the beam travels down successively the two linacs and thus, the low energy part becomes the high energy part in one of the linacs. The first linac is unchanged, but in the second one, the quadrupole spacing of 4 modules is conserved, while the quadrupole spacing of 3 and 2 modules is enlarged to 6 modules. A schematic drawing of the beam optics for the three energies is represented on Fig.3.3.2. Table 3.3.1 sums up the maximal integrated field gradients, assuming a constant phase advance of 60 degrees.

	TESLA 500	TESLA 800	TESLA 1600
Linac energy (GeV)	250	400	800
Quad spacing (modules)	2-4	2-4	2-6
Max int. gradient (Tesla)	17	27	36

Table 3.3.1: *Maximum integrated gradient for the main linac upgrades.*

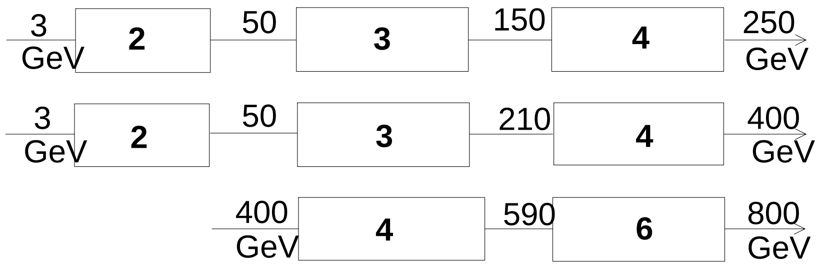

Figure 3.3.2: *Quadrupole spacing (in unit of cryo-modules) for the TESLA linac upgrades.*

3.3.3 Emittance Preservation

To achieve very flat and tiny beams at the collision point, beams of very small emittances, especially in the vertical plane, must be first generated by the injector and second accelerated by the main linac, while preserving the high quality beam to the final focus system. Since the beam pulse is composed of many bunches, single bunch and multibunch effects must be studied. Once the tolerable emittance growth is specified, all the tolerances on the various errors, like injection jitter and misalignment of the linac components, i.e. accelerating structures, focusing magnets and beam position monitors, can be in principle determined. Simple analytical expressions can help to estimate the individual tolerances. However, the net effect of simultaneous errors in a real machine is not the simple summation of the individual effects of the errors, therefore numerical simulations must be performed. The emittance growth was studied with the tracking code DILEM, which simultaneously combines single and multibunch effects of multiple errors and includes numerous correction techniques, like simple and elaborated orbit steering or wakefields compensation methods.

3.3.3.1 Single Bunch Effects

We consider first the short-range wakefield effects: As a bunch travels down accelerating structures, wakefields are excited and will act back on the bunch itself. The longitudinal wakefields affect the energy of the particles along the bunch, whereas for off-axis beam trajectories, the transverse wakefieds tend to deflect the beam further away from the axis. The deflection is stronger for the trailing particles, giving rise to a "banana shape" of the bunch and an increase of the transverse emittance.

Longitudinal single bunch dynamics

Though not easy for short bunches - bunch length smaller than 1 mm - passing through TESLA 9-cell cavities, the longitudinal wakes were carefully computed. Furthermore, since the beam tubes, larger than the iris openings, which connect two adjacent cavities, form themselves also cavities, a chain of at least 5 cavities is necessary to get the convergence of wake computation for a 0.7 mm long bunch, as we can see in Fig. 3.3.3. In addition to the final longitudinal bunch potential, computed for a chain of 8 cavities and normalized for 1 cavity, the individual wakes, induced in each of subsequent cavities in the module, are plotted as a function of the axial position in the bunch (head of the bunch is on the right side). A bunch, travelling through the accelerator, will gain energy from the externally driven accelerating mode and will lose energy due to the longitudinal wakefields. The net energy spread can be reduced by running the bunch off the crest of the accelerating wave, such that the RF wave slope tends to cancel the average slope of the beam induced potential. As we will see thereafter, the BNS damping technique, which uses additional correlated energy spread to reduce the transverse wakefield effects on a bunch performing a betatron oscillation, is not needed in the TESLA linac. Minimal energy spread can then be achieved all along the linac by running the bunch at the optimal phase. For the parameters of TESLA 500, the optimal phase is 3.4 degrees, leading to a final correlated energy spread lower than 5.10^{-4}. Fig. 3.3.4 shows the energy variations due to the longitudinal wake, the RF wave and the sum of both contributions within the bunch. Bunch charge fluctuations are not critical: for a 10 % charge variation, the bunch energy spread still remains well below 10^{-3}. In addition to this correlated energy spread induced by the structures of the main linac, the energy spread of the injected beam, generated by the injector, and decreasing adiabatically with the energy, is taken into account in all the simulations, with an initial value of 1%.

Transverse single bunch dynamics

For beam dynamics studies in the transverse plane, we need the transverse delta wake excited by a point-like bunch, while cavity codes give only the transverse bunch wake of a displaced bunch. Fig. 3.3.5 shows the transverse impulse factor $k_\perp$, quantity proportional to the total transverse momentum given to the bunch by its own wake, computed for different bunchlengths. A fit of $k_\perp$ suggests a $\sigma^{1/2}$ asymptotic dependance. The corresponding delta wake per cavity, and used for single bunch instability calculations, is directly deduced from the fit of the transverse impulse factor,

$$W_\perp(s) = 1290\sqrt{s} - 2600\,s \qquad (\mathrm{V/pC/m})$$

where s is the position with respect to the exciting point-like charge. When a beam is injected off-axis, performing a betatron oscillation about the central orbit, the tail particles are driven on resonance by the wakefield excited by the head particles and the amplitude of the oscillation grows dramatically as the beam proceeds down the linac. This resonant effect leads to a tight tolerance on the amplitude of the betatron oscillation, unless BNS damping is used to cure this resonant effect. By making the head more energetic than the tail of the bunch, the transverse wake effect is then partially compensated by the chromatic phase advance of the trailing particles. However, the bunch energy spread is then larger, giving rise to a larger dispersive dilution, due to

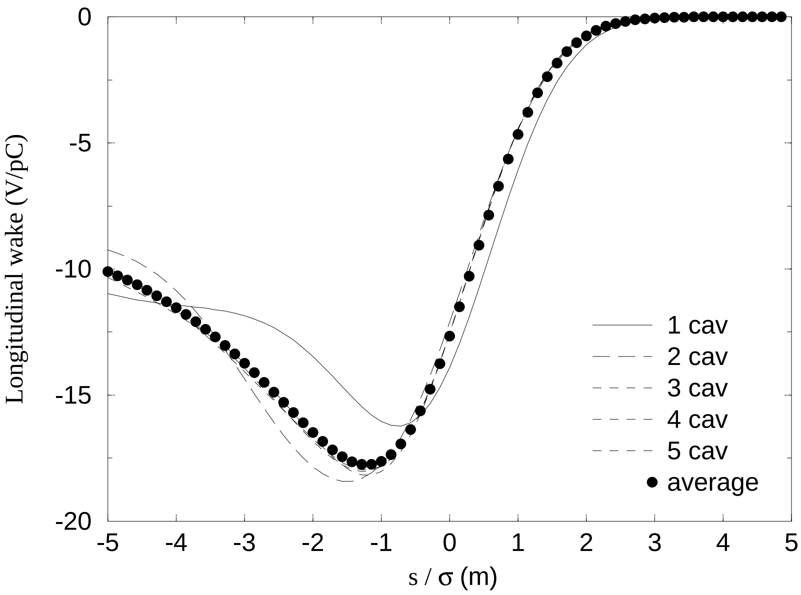

Figure 3.3.3: *Longitudinal bunch wake potentials induced in each of the subsequent TESLA cavities in a module (bunchlength σ = 0.7 mm)*

quadrupole misaligments. Thanks to the low wakefields of the TESLA cavities, BNS damping is not necessary and the energy spread can then be kept to its minimal value all along the linac. Fig. 3.3.6 shows the development of the emittance growth along the linac for the TESLA 500 lattice, assuming an initial beam offset equal to a full rms beam size and no BNS damping. We note that even for this large beam jitter, the final emittance growth is lower than 6%. The transverse wakefields driven by random misalignments of the cavities will deflect the beam from side to side around the central axis. The two particle model, describing the bunch by two macro particles, two bunchlengths spaced, gives an analytical expression of the final emittance growth at the linac exit

$$\frac{\Delta\varepsilon}{\varepsilon} \propto \frac{N^2 W_\perp^2}{\varepsilon} \beta_\mathrm{o} \frac{1}{\alpha} \left[\left(\frac{\gamma_\mathrm{f}}{\gamma_\mathrm{i}} \right)^\alpha - 1 \right] y_\mathrm{c}^2$$

where y_c denotes the rms offset of the cavities, N the bunch population, $W_\perp$ is the transverse wake evaluated at 2 σ_z, β_o the beta function at the linac entrance and α the exponent of the beta scaling with energy, normally set between 0 and 1/2. We note that the more the beam is focussed (β_o and α small), the less the beam is diluted by the wakefields.

In order to avoid a continually growing trajectory in presence of quadrupole position errors, the beam must be steered all along the linac. The simplest trajectory correction is the 'one-to-one' correction, in which the dipole correctors steer the beam towards the quadrupole centers after reading of the BPM measurements. Since the actual orbit will then follow the BPM misalignments, significant dispersive errors will arise. Once again, a two particle model can be used to find an analytical estimation of the

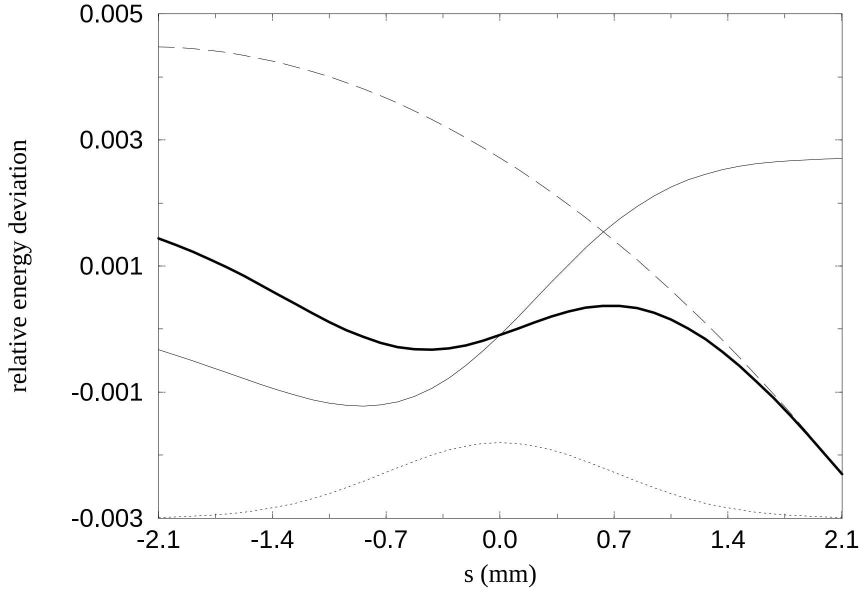

Figure 3.3.4: *Energy profiles within the bunch due to longitudinal wake (thin line), RF wave (dashed line) and both effects (thick line). The dotted line denotes the Gaussian bunch profile.*

emittance growth. For example, for a correlated energy spread, the emittance growth can be written as

$$\frac{\Delta\varepsilon}{\varepsilon} \propto \frac{\delta_c^2}{\varepsilon}\frac{1}{\beta_o^2}\frac{1}{1-\alpha}\left[\left(\frac{\gamma_f}{\gamma_i}\right)^{2-2\alpha} - 1\right] y^2$$

where δ_c is the relative rms correlated energy spread, y is the rms offset of the BPMs (including quadrupole offset and BPM offset relative to the quadrupole center). Contrary to the previous dilution driven by the cavity misalignments, the dispersive emittance dilution is lower for a less focussed beam (β_o and α large). An optimal focusing lattice, in which the dispersive effects and the wakefield effects are balanced, can then be found. Fig. 3.3.7 shows for example the vertical emittance growth, due to simultaneous chromatic and wakefields effects, driven by random quadrupole and cavity alignment errors, with different scalings of the beta function with energy. The rms quadrupole, BPM and cavity offsets are $\sigma_q = 100\ \mu m$, $\sigma_{bpm} = 100\ \mu m$ and $\sigma_c = 500\ \mu m$, respectively. We conclude that a small beta scaling, $\alpha = 0$ to 0.2, provides the smallest emittance dilutions. The mean emittance growth, computed with the chosen TESLA 500 lattice, the same misalignments and the simple "one-to-one" correction, is 12%. To alleviate the dispersive dilution, more elaborated correction algorithms have been proposed. All these methods refer to beam based alignment (correction) techniques, because the magnet misalignments (corrector settings) are deduced from BPM measurements with different beam trajectories. For example, the "shunt" technique consists in moving each quadrupole until no beam shift is observed at the next BPM or

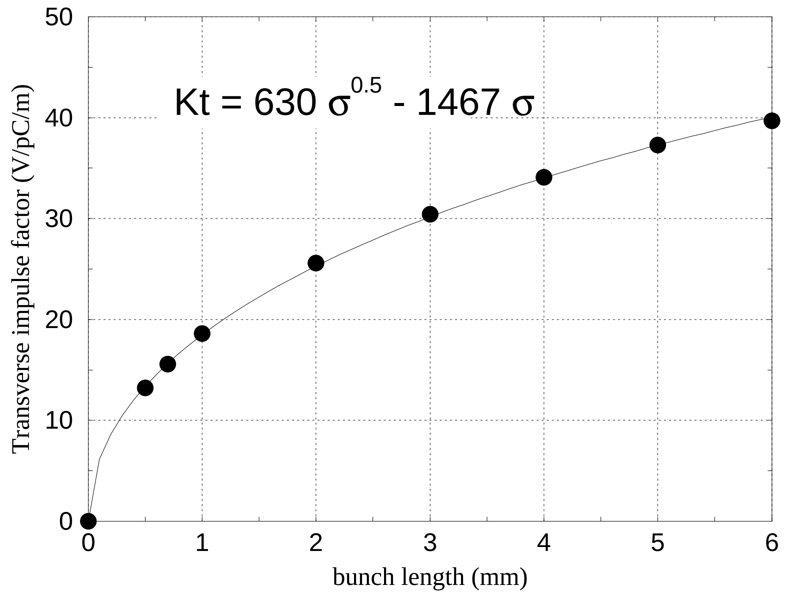

Figure 3.3.5: *Transverse impulse factor $k_\perp$ per cavity for different bunchlengths.*

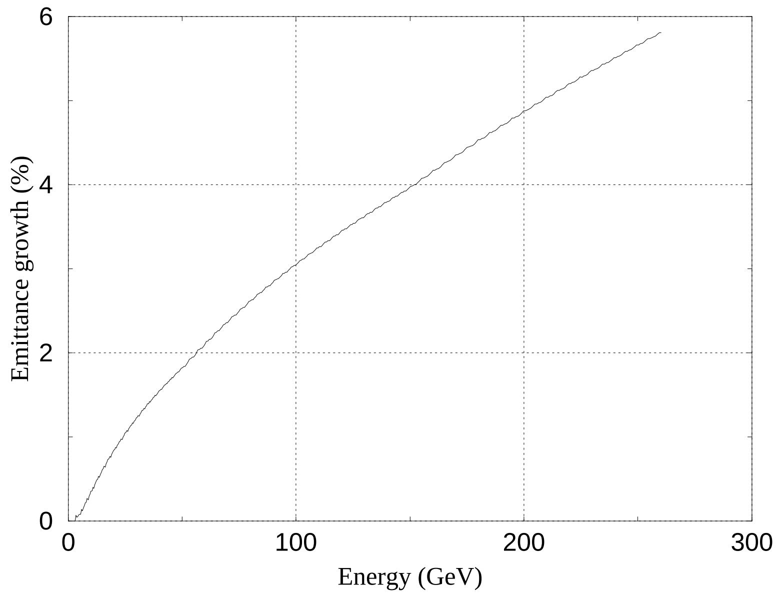

Figure 3.3.6: *Vertical emittance growth with a beam offset equal to the rms beam size.*

the 'Dispersion Free' correction, where at least two trajectories with effective different energies are used to cancel the dispersive errors. In this case, the final dispersive error is much less dependent of the magnitude of the misalignments, but is still limited by the BPM resolution, the reading-to-reading jitter of the BPM measurement. With the help of these beam based corrections, which could be applied after some machine

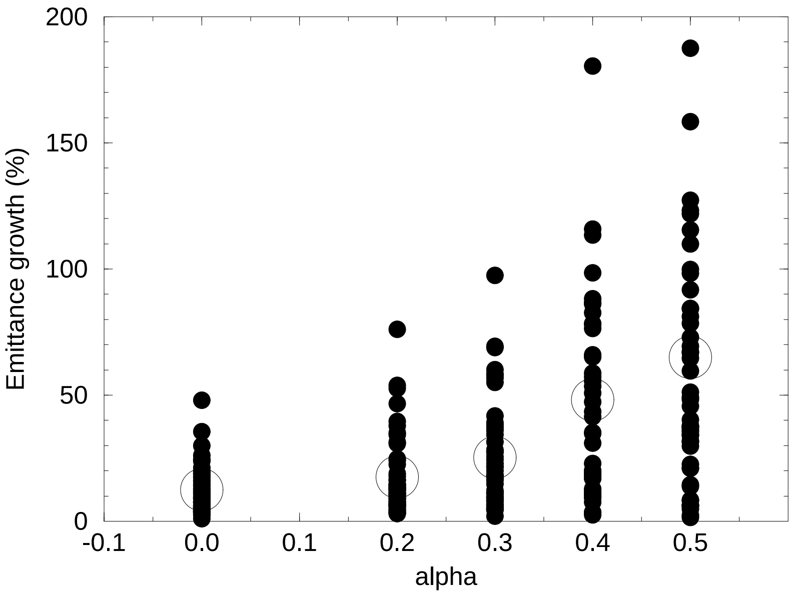

Figure 3.3.7: *Emittance growth vs. beta scaling parameter a with energy.*

experience, the tolerance on quadrupole misalignment can, of course, significantly be relaxed. For example, let now quadrupole alignment errors be equal to the cavity ones ($\sigma_q = \sigma_c = 500\ \mu m$), the tolerance on the BPM resolution is $\sigma_{res} = 15\ \mu m$ by using the "shunt" correction technique.

For correlated errors, the dispersive dilution depends on the correlation length of alignment errors. For example, Fig. 3.3.8 gives the quadrupole tolerance as a function of the wavelength, without wakefield effects and assuming an energy spread of 5.10^{-4}. We note that for small wavelengths, the tolerance of 100 μm, corresponding to random errors, is recovered whereas for the long wavelength components the tolerance is much looser. In addition to a position error, the cavity can be tilted with respect to the horizontal beam line and the accelerating field gives an additional transverse kick to the beam, with a strength which depends on the longitudinal position along the bunch. The tolerance on this cavity angle error has been estimated at 1 mrad from numerical simulations.

3.3.3.2 Multi Bunch Effects

The TESLA beam pulse is composed of many bunches, which will feel the long-range wakefields of all the preceding bunches and will be more and more deflected as they proceed down the linac. This phenomenon, called multibunch beam breakup, would require to place the cavities very precisely with respect to the beam axis. In addition, similar to the single bunch dispersive dilution, the bunch-to-bunch energy deviation will introduce a multibunch beam filamentation.

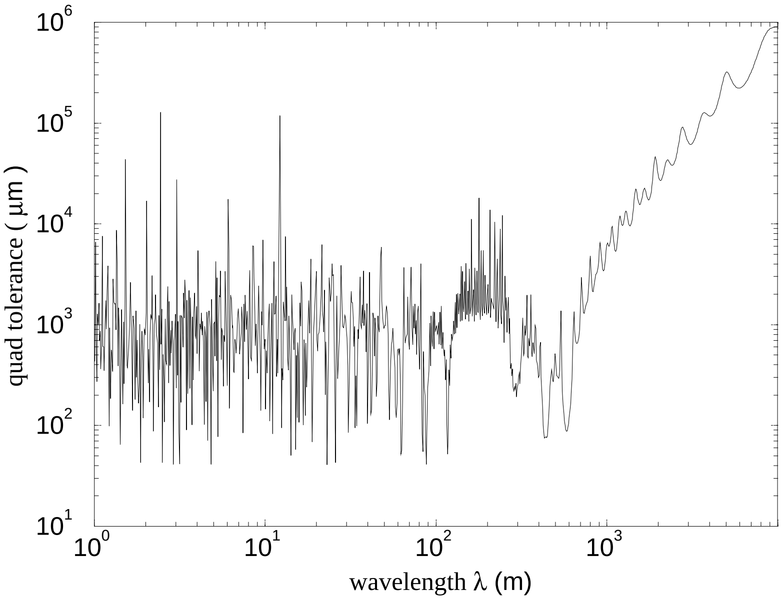

Figure 3.3.8: *Quadrupole alignment tolerance vs. wavelength for a 3% dispersive emittance growth with an energy spread of* 5.10^{-4}.

Longitudinal multi-bunch dynamics

The inter-bunch energy spread has to be smaller than the intra-bunch energy spread in order to preserve the transverse beam quality from chromatic effects. In particular, an 'optimal' trajectory (also called a 'gold' trajectory) for the first bunch of the train, giving the smallest single bunch emittance dilution, as discused above, will be lost for the following bunches if the bunch to bunch energy deviation is too large. This multibunch energy spread is mainly produced by the transient beam loading in the accelerating structures. Fortunately, the high beam loading will be compensated in the standing-wave TESLA cavities by matching the power extracted by the beam to the RF power supplied by the klystron. The residual energy gain variations along the beam pulse, caused mainly by Lorentz forces or microphonics detuning and RF mismatches, will be suppressed by the feedback system down to a few 10^{-4}. The extra power required for the field stabilization, of the order of 10%, could be strongly decreased with the help of harmonic cavities installed at a few locations along the linac. The systematic energy fluctuations would then be locally cancelled, in such a way that the beam filamentation has no time for growing.

On the other hand, the different energy kicks, imparted to the bunches of the train by the longitudinal higher order modes, cancel out because of the natural frequency spread of the modes, and are therefore harmless.

Transverse multi-bunch dynamics

With a train of bunches, the long-range wakefields excited by each bunch will act on the subsequent bunches. The major effect comes from the multibunch beam break-up (or cumulative BBU) : a beam passing off-axis through an accelerating structure excites transverse dipole modes, causing transverse deflections of the following bunches. This displaced beam will excite similar modes in the downstream structures, which will, in turn, deflect even more the following bunches of the train, and so on, resulting in an increase of the beam emittance. To suppress the cumulative BBU, the conjunction of two cures are used, namely the detuning and the damping techniques. Unlike long normal conducting sections with many cells, where the detuning usually takes place inside each structure, the deflecting modes frequencies change from cavity to cavity over the whole linac. The Gaussian detuning is naturally provided by the fabrication errors. The effective wake is then the average of the individual wakes over many structures, as long as the bunch displacement is small. For a Gaussian distribution and an infinite number of cavities, the wake would be reduced by the factor $\exp\left[-1/2(\sigma_\omega\tau)^2\right]$, where σ_ω and τ are the rms angular frequency spread and the time slipped away. In reality, the averaging is performed over a finite number of sections and the wake envelope does not vanishes, due to the recoherence effect. In order to reduce the effective wake for the rest of the long TESLA bunch train, a slight damping is necessary. The lower the quality factor Q, the less the excited field will persist over the bunchtrain. The quality factors of the modes are reduced by means of higher order modes dampers, which are mounted at both ends of the TESLA cavity. The parameters used for the multibunch calculations - frequency, geometric impedance and Q - of the ten most dangerous dipole modes are shown in Table 3.3.2. The assumed dampings, Q values of around or below 10^5 for the highest R/Q modes are in agreement with measurement on copper models. The effective dipole wake, resulting from the detuning and damping effects, is plotted

Frequency (GHz)	R/Q Ω/m^2	Q_{loaded}
1.874	$8.61\ 10^4$	$1.20\ 10^5$
1.865	$6.38\ 10^4$	$7.56\ 10^4$
1.880	$1.92\ 10^4$	$1.94\ 10^3$
1.736	$1.48\ 10^5$	$7.20\ 10^3$
1.887	$1.60\ 10^3$	$6.73\ 10^5$
1.709	$1.14\ 10^5$	$8.40\ 10^3$
1.837	$5.00\ 10^3$	$4.68\ 10^4$
1.884	$5.00\ 10^2$	$3.31\ 10^5$
1.853	$3.00\ 10^3$	$5.16\ 10^4$
1.763	$1.70\ 10^4$	$7.20\ 10^3$

Table 3.3.2: *Parameters of dipole cavity modes.*

on Fig. 3.3.9. The theoretical wake and the more realistic wake, when averaged on the finite number of cavities over a few betatron wavelengths, and assuming no damping at all, are also shown for comparison. Thanks to the modes detuning, the dipole wake decreases by a factor of 12 with respect to the peak value when the second bunch comes (0.7 ms later) and by a factor of about 90 for the other bunches. Though the mode damping does not provide a significant additional reduction factor on the second bunch, it is, on the other hand, very efficient for the end of the bunch train. In other words, thanks to the large bunch spacing and the natural mode detuning, a weak damping is sufficient for preserving the beam quality of the whole bunch train. The multi-bunch emittance growth for the whole train can be computed for different

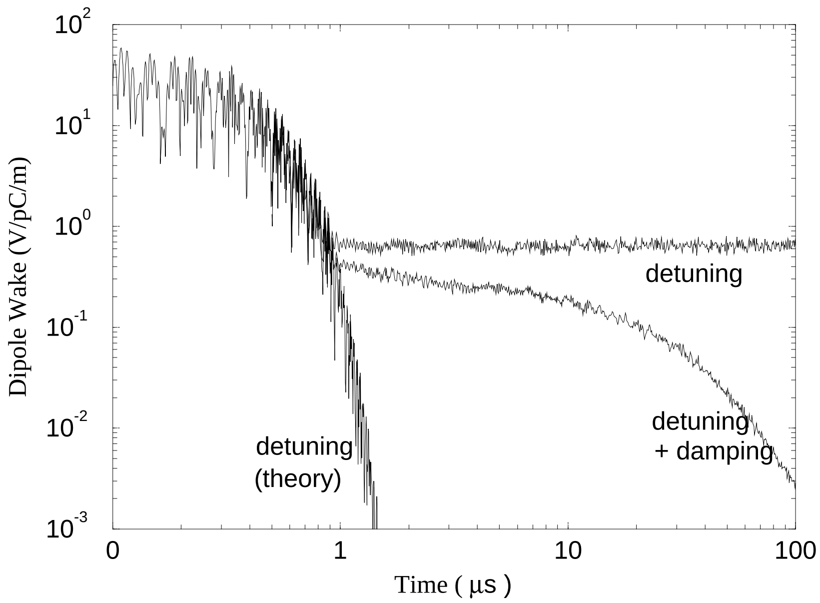

Figure 3.3.9: *Theoretical and real effective dipole wake, without and with damping.*

damping levels. It is shown on Fig. 3.3.10, as a function of the scaling factor by which the real Q of all the dipole modes of the TESLA cavity have been multiplied. For these calculations with the lattice of TESLA 500, an inter-bunch energy spread of $3.5 \cdot 10^{-4}$ is taken into account, the simple 'one-to-one' trajectory correction is applied and the quadrupole and cavity alignment tolerances, specified by single bunch dynamics (σ_q = 100 μm and σ_c = 500 μm) are chosen. The mean value of the emittance growth is only few percents for the real Qs (scaling factor = 1) of the cavity modes. This low multi-bunch dilution prevents any further dilution of the single bunch emittance. Calculations, including simultaneous single and multi-bunch effects, confirmed that the overall emittance dilution for the whole bunch train is very close to the single bunch emittance dilution. Once the multi-bunch beam break up has been well controlled, the beam energy has to remain as stable as possible to prevent any further filamentation.

In case of klystron trips, especially in the low energy part of the linac, the relative energy variation can be large (32 cavities are fed by one klystron) leading to a large beam orbit variation. However, thanks to the orbit feedback, the initial orbit can be rapidly recovered after a few beam pulses.

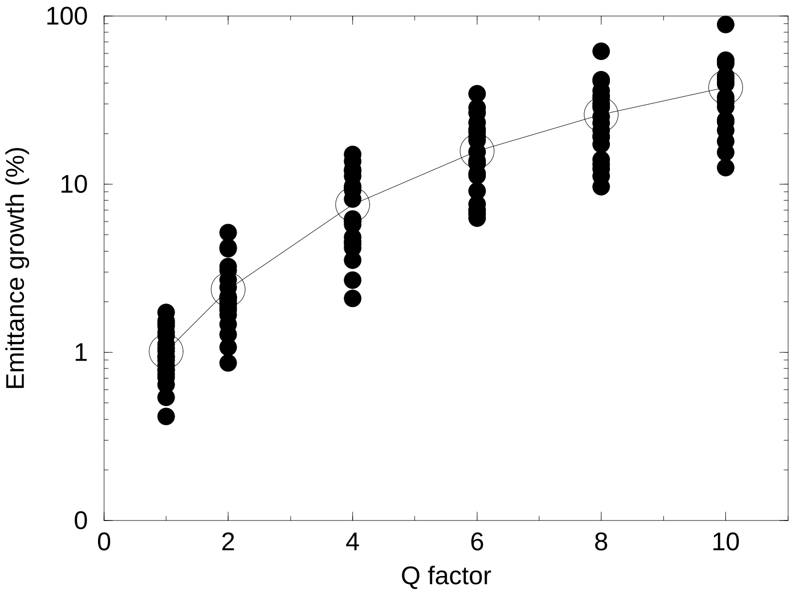

Figure 3.3.10: *Multi-bunch emittance growth as a function of the damping level (TESLA 500 lattice, σ_q = 100 μm and σ_c = 500 μm).*

3.3.4 Orbit Stability

Ground motion is of major concern because it will displace focusing magnets, which, in turn, will dilute the beam emittance in the linac through dispersive effects. Numerous power spectra of ground motion have been measured at different places. At low frequency, the motion can be quite large and is usually described by the 'ATL' law. Beam orbit feedback, involving dipole correctors and BPMs, can be used, at least up to a frequency of about $f_{rep}/20$, corresponding to 0.25 Hz for TESLA. At high frequency, the motion falls off rapidly, but is too fast to use beam orbit feedback with simple steering magnets.

The diffusive ground motion, leading to large displacements after long time intervals, can be described by the 'ATL' law, which states that the relative rms displacement Δy after a time T of two points separated by a distance L is given by

$$\Delta y_{rms}^2 = A \cdot T \cdot L$$

The parameter A ranges from 10^{-7} to 10^{-5} $\mu\text{m}^2/\text{s}/\text{m}$, depending on the site. Beam-based alignment techniques will recover either the proper alignment of the elements or the 'gold' trajectory, this one which minimizes the dispersion. Nevertheless, these dispersion free corrections require measurements of the beam orbit with different quadrupole settings can only be used periodically, with some rather long time intervals. In between, correction feedback loops have then to steer the beam continuously to the original gold orbit such as it was previously measured by the BPMs. Fig. 3.3.11 shows the resulting emittance growth as a function of the product $A \cdot T$. We note that the diffusive ground motion produces a linear growth of the dispersive dilution with time. Limiting a maximal emittance growth to 15% and assuming a conservative value of the parameter $A = 10^{-5}$, the beam orbit must be re-steered about once per hour, a very comfortable value for the cut-off frequency of 0.25 Hz of the beam orbit feedback. With correctors steering periodically the beam to the original orbit, the quadrupole displacements are so large after a long time that a new gold trajectory must be found again by means of a beam base correction technique. Assuming again a tolerable emittance growth of 15%, the time interval between two such procedures, which necessary stops the physics experiments for a few hours, is several years. Fast vibrations, or jitter in quadrupole

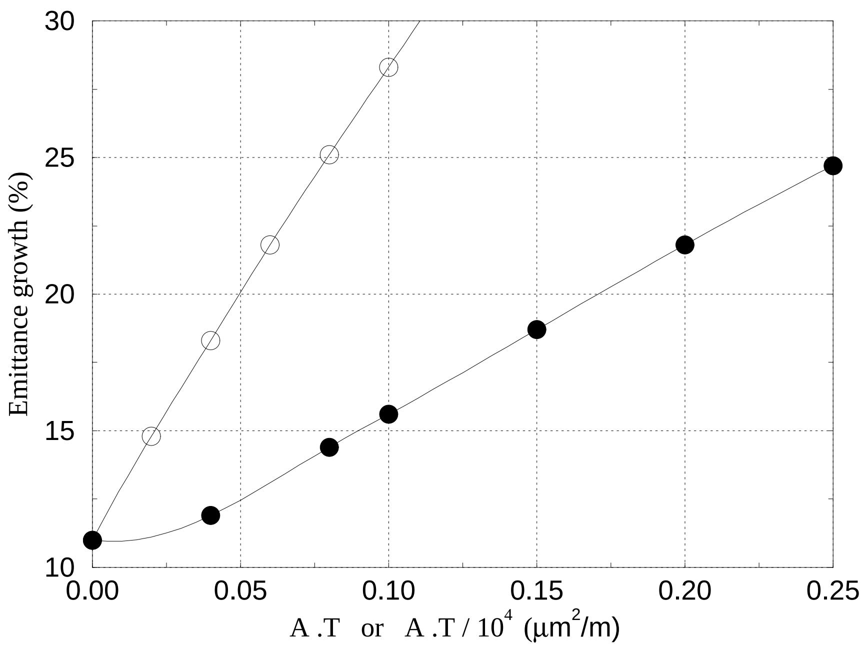

Figure 3.3.11: *Averaged emittance growth vs. time for diffusive ground motion without (white circles) and with orbit feedback (black circles).*

position, cannot be compensated by conventional dipole correctors and will scatter the bunch centroids at the end of the linac, thus preventing the bunches from colliding at the interaction point. Allowing a maximum luminosity reduction of 3%, the rms amplitude of the fast quadrupoles motions we could tolerate can be written as

$$y_{qrms}^2 = \frac{\varepsilon_y}{16} \frac{\overline{\beta}_f^2 \, sin\mu \cos^2\mu/2}{4L_{\rm tot}} \, 2\,(1-\alpha)$$

where α is the exponent of the beta scaling with energy. With the lattice of TESLA 500, the jitter tolerance would be about 80 nm. Fortunately, since the bunches within the train have very large spacing, feedback can be applied on the bunch centroids within the train. The fast kickers at the end of the linac will re-align the bunches, after reading the displacement of the first several bunches. In addition to this bunch offset problem at the exit of the linac, the deviation of the bunch trajectories from the normal corrected orbit will induce beam filamentation, through dispersive effects. In this case, the tolerance on quadrupole jitter is about 1 μm, larger than the expected displacements at high frequency.

3.3.5 Summary Tolerances and Emittance Dilution

Beam dynamics studies allowed to find an optimized focusing lattice, for which the wakefield and dispersive effects are balanced, and to estimate the final emittance dilution for given tolerances. The initial alignment of the elements, with a tolerance on both cavities and quadrupoles of the order of 500 μm, can be accomplished by a conventional survey. In case of the quadrupoles and the BPM's w.r.t. the quadrupoles, the expected accuracy is actually smaller, about 0.1...0.2 mm. Later on, there is no need to move any quadrupole or cavity for re-alignment. Estimations of beam dilution with the simple 'one-to-one' orbit steering point out that the quadrupole and BPM offsets must then be located within a 100 μm range. Even if slightly exceeded at installation time, this tolerance can be easily achieved with the help of beam based correction procedures and was already met on the SLC at Stanford with BPM resolutions of about 15 μm. For example, numerical simulations, showed that the 'shunt' technique, which locally cancels the dispersion by varying the quadrupoles one-by-one, without requiring neither linac modelling nor matrix computations, restrict the bunch emittance growth to 10% with the same BPM resolution of 15 μm. The expected BPM-resolution is better than that and more advanced beam-based methods can be applied, so that it will be possible to achieve a smaller emittance dilution than required for the TESLA design parameters.

With regard to the energy upgrades of the main linac to 400 and 800 GeV (TESLA 800 and TESLA 1600), the emittance growths amount to about 20% for the same cavity and quadrupole tolerances.

Thanks to large bunch spacing and to strong reduction of the transverse wake, due to complementary effects of natural cavity-to-cavity detuning and of slight mode damping, the multibunch beam breakup is well controlled. Assuming an inter-bunch energy spread lower than $5 \cdot 10^{-4}$, the multibunch emittance growth is much smaller than the single bunch one. For that reason, tracking calculations involving single and multibunch effects give very similar results to those solely involving single bunch effects.

For slow ground motion, feedback loops adjust the beam orbit to the 'optimal' trajectory, previously found by beam based correction. According to the phenomenological 'ATL' law, predicting the relative displacement with time and position, the steering feedback has only to be faster than one hour. When the elements displacement becomes too large, beam based correction can be used again, every few years. For fast motion, fast deflecting correctors, located at the linac end, will be used to re-align the bunch centroids. The tolerance on quadrupole jitter is then simply determined by the dispersive errors arising through the linac and is of the order of one micron.

Bibliography

[1] V. Balakin, A. Novokhatski, V. Smirnov, *VLEPP: Transverse Beam Dynamics*, Proc. 12^{th} Int. Conf. on High Energy Accelerators, Fermilab, 119 (1983).

[2] T. Raubenheimer, *The Generation and Acceleration of Low Emittance Flat Beams for Future Linear Colliders*, SLAC-387 (1991).

[3] B. Baklakov, P. Lebedev, V. Parkhomchuk, A. Sery, A. Sleptsov, V. Shiltsev, *Investigation of Seismic Vibrations and Relative Displacement of Linear Collider VLEPP Elements*, Proc. 1991 Part. Accel. Conf., San Francisco, 3273 (1993).

[4] A. Mosnier, *Instabilities in Linacs*, CERN Accel. School, Rhodes, CERN 95-06, 459 (1993).

[5] A. Novokhatski, A. Mosnier, *Short Bunch Wake Potentials for a Chain of TESLA cavities*, Int. Report, CEA Saclay, DAPNIA/SEA-9608 (1996).

[6] A. Mosnier, *Beam Instabilities Related to Different Focusing Schemes in TESLA*, Proc. 1993 Part. Accel. Conf., Washington, 629 (1993).

[7] A. Mosnier, *Single and Multi-bunch Wakefields Effects in the TESLA Linac*, Proc. 4^{th} European Part. Accel. Conf., London, 1111 (1994).